Photothermal Gas Detection Using a Mode-Locked Laser Signal Readout

Karol Krzempek, Piotr Jaworski, Piotr Bojęś, and Paweł Kozioł

***Abstract*—In this work, a novel configuration of a photothermal gas sensor is demonstrated. The measured gas sample is delivered to a gas cell placed inside the linear cavity of a 1.55 μm mode-locked fiber laser. The gas refractive index modulation resulting from the excitation by an auxiliary continuous wave laser is efficiently probed by analyzing the phase shift of the self-heterodyne beatnote signal of the mode-locked laser. IQ demodulation combined with Wavelength Modulation Spectroscopy-based signal analysis was employed to optimize and simplify the spectroscopic data acquisition and analysis. A proof-of-concept experiment with detection of carbon dioxide at 2 μm wavelength yielded a noise equivalent absorption of $2.25{\cdot}10^{-7}$ for 1000 s integration time. The proposed sensor configuration is versatile and can be used to probe any gas molecule, provided an appropriate excitation source is used to induce the photothermal effect.**

***Index Terms*—Laser spectroscopy, mode-locked laser, photothermal spectroscopy, wavelength modulation spectroscopy (WMS).**

I. Introduction

LASER-BASED gas detection techniques are undergoing relentless development, which is fueled by the rapid technology advancement observable in all industry sectors. Precise, selective and in-vivo monitoring of gas particles is essential not only in the manufacturing and environmental protection, but also in newly-emerging medical and military applications [1]. New configurations of gas sensors and the required spectroscopic signal processing techniques were discovered only by the development and ongoing improvement of compact, power efficient and robust mid-infrared (mid-IR) lasers, i.e., quantum cascade lasers (QCLs) and interband cascade lasers (ICLs), which enabled accessing strong transitions of gas molecules in this particular wavelength region. Mitigating the requirements for constructing nonlinear frequency conversion-based coherent sources, which are known for their complexity, mid-IR gas sensors managed to find out-of-lab applications as commercial products [2]. However, accessing the strong absorption lines of gas molecules in the mid-IR generally comes at the cost of integrating expensive detectors, which can efficiently probe the required parameters of the light interacting with the measured gas samples. Mercury cadmium telluride (MCT) detectors are commonly used for such purposes, yet, the environmentally and health harmful elements required for their manufacturing stimulate researchers to develop alternative devices for detecting the mid-IR radiation. The substitute technologies to MCT detectors are yet to be fully verified in the years to come. These for example include novel superlattice detectors based on indium arsenide and gallium antimonide structures [3]–[5].

The abovementioned limitations lead to the development of sensor configurations, which allow obtaining superb gas detection sensitivities, while relying on optical signal recovery based on well-developed and cost-effective components and devices, mostly near-infrared (near-IR) detectors. Unfortunately, not all gas molecules have strong fingerprint spectra in the 1 μm to 2 μm wavelength region, therefore clever techniques combining the advantages of using mid-IR lasers as the excitation sources, with the simplicity and cost effectiveness of using near-IR detectors and optics have been developed. One of such methods relies on the photothermal effect, which can be induced in solids, liquids and gases [6]. Firstly demonstrated in [7], photothermal spectroscopy (PTS) of gases is nowadays re-invented, and thus can show its full potential with the development of precise optics, low-noise near-IR detectors and non-standard approach to spectroscopic signal retrieval combined with highly efficient de-noising and processing techniques.

In PTS the gas molecules are excited with a light source with a wavelength matching their particular absorption line – called the *pump*. The excited particles return to their steady state mostly via non-radiative collision energy transfer, which creates a localized temperature gradient in the sample, protruding along the pathlength of the *pump* laser. The temperature gradients translate to confined variations of the gas density, which can be observed also as changes in its refractive index (RI). Most of currently demonstrated PTS-based gas sensors rely on the principle of probing the RI modulations with an auxiliary laser, the so-called the *probe*. The main and unique feature of the PTS-based gas sensing technique relies on the possibility of separating the *pump* and the *probe* parts of the setup, and thus, each can be precisely tailored for its particular function. This directly translates to the possibility of registering the spectroscopic signal using cost-effective and easily available near-IR laser and detectors, while the gas molecules can be excited by

Manuscript received November 8, 2021; revised January 26, 2022; accepted February 20, 2022. Date of publication March 1, 2022; date of current version July 2, 2022. This work was supported by the National Science Centre, Poland, M-ERA.NET 2 Call 2019 under Grant 2019/01/Y/ST7/00088 and SONATA15 under Grant 2019/35/D/ST7/04436. *(Corresponding author: Karol Krzempek.)*

The authors are with the Faculty of Electronics, Photonics and Microsystems, Laser Spectroscopy Group, Wroclaw University of Science and Technology, 50-370 Wroclaw, Poland (e-mail: karol.krzempek@pwr.edu.pl; piotr.jaworski@pwr.edu.pl; piotr.bojes@pwr.edu.pl; pawel.koziol@pwr.edu.pl).

Color versions of one or more figures in this article are available at https://doi.org/10.1109/JLT.2022.3155354.

Digital Object Identifier 10.1109/JLT.2022.3155354

sources operating, e.g., in the mid-IR spectral band, taking the full advantage of strong absorption lines. However, the difficulty of employing the PTS principle for gas detection lies in the miniscule amplitude of the induced RI variations. The ambition of obtaining satisfactory detection limits lead to the development of several unique configurations of PTS gas detectors. Majority of the reported up to date sensors rely on interferometric signal retrieval, which provides the required RI modulation readout sensitivity. Those can be split into two main groups: based on Fabry-Perot (FPI) and Mach-Zehnder interferometer (MZI) configurations. In that case the RI change is translated to a phase change $\Delta\theta$, which can be expressed as follows [8]:

$$\Delta\emptyset = k\alpha\left(\lambda_{pump}\right) CLP_{pump} \tag{1}$$

where C is the gas concentration, $\alpha(\lambda_{\mathrm{pump}})$ is the absorption coefficient at the *pump* wavelength, L is the length of the modulated region, P_{pump} is the *pump* power of the laser inducing the RI modulation. The k parameter depends on the gas parameters, modulation frequency of the *pump* light and its beam parameters. The phase modulation amplitude is linearly dependent on the gas molecules concentration, the *pump* power and the length of the gas-laser interaction path, thus can be conveniently used to determine the concentration of the target mixture.

Numerous PTS gas sensor configurations have been presented up to date. These included bulk optics-based interferometric sensors [9]–[12], intracavity sensors [13], [14] and more sophisticated fiber-based gas detectors with superb sensitivity [8], [15]–[19]. Configurations based on the use of hollow-core fibers (HCF) in most cases provide excellent sensitivity (even down to a minimum absorption coefficient of 10^{-11}) but at a cost of using complex optical layouts, sophisticated stabilization feed-back loops, require using specially coated optics to ensure high Finesse of the cavity, or are limited to working in the near-IR wavelength range.

The work presented in this paper documents further development of an unique approach to probing the photothermal-induced (PT) gas RI modulation, which uses the self-heterodyne signal of a mode-locked (ML) fiber laser working in the 1.55 μm wavelength range [13]. In this paper, the improvement in the ML laser cavity configuration and the signal processing methods were investigated, yielding a substantial enhancement of its performance. The proposed approach to PT-induced signal readout is unique and significantly dissimilar compared to numerous previously published configurations, where the spectroscopic signal is encoded in amplitude variations due to the continuous wave (CW) interferometric nature of the readout [11], [17], [20]–[22]. In our proposed PTS sensor, the gas particles under test are enclosed in a gas cell, which is a part of a standard linear cavity fiber ML laser. The excitation of the gas via the auxiliary *pump* laser and the resulting RI modulation affects the optical path-length of the ML laser. This allowed us to exploit the possibility of non-complex, direct translation of the gas concentration information to frequency deviations of the ML self-heterodyne beatnote, mitigating problems related to purely amplitude-based signal readout. The signal processing was simplified by employing IQ demodulation of the frequency deviations along with Wavelength Modulation Spectroscopy (WMS) detection technique. The sensor layout is non-complex, built using off-the-shelf polarization maintaining (PM) fibers and a minimum number of bulk optics components. The re-designed and improved original PTS gas sensor is not only less complex, but also an order of magnitude more sensitive when compared to its previous version reported in [13].

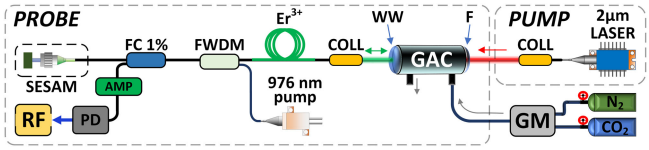

Fig. 1. Experimental setup. SESAM – fiber pigtailed semiconductor saturable absorber mirror, RF – RF spectrum analyzer, PD – photodiode, AMP – erbium doped fiber amplifier, FC – fiber coupler with 1% out-coupling ratio, FWDM – filter-type wavelength division multiplexer, Er^{3+} - 30-cm-long erbium doped fiber, COLL – fiber collimator, WW – wedged window, F – long-pass optical filter, GAC – 20 cm-long gas absorption cell, GM – gas mixer.

II. Experimental Setup

The experimental setup of the sensor is depicted in Fig. 1. The core of the PTS gas sensor is a standard configuration of a linear cavity ML laser working in the 1.55 μm wavelength region. The ML laser serves as the *probe* in this sensor. The longitudinal mode synchronization is achieved by incorporating a semiconductor saturable absorber mirror (SESAM; BATOP, SAM-1550-30-2ps), glued directly to a ferrule of a fiber connector. A 30 cm-long piece of erbium-doped fiber (Liekki Er80) was used as the gain medium, which was optically pumped by a singlemode laser diode ($\lambda = 976$ nm) via a filter-type wavelength division multiplexer (FWDM). The second mirror of the ML laser cavity was a long-pass filter (F; Thorlabs, DMLP1800), which was mounted on the far end of a self-made, 20 cm-long gas absorption cell (GAC). The free-space optical path required for including the GAC in the ML laser cavity was established by outcoupling the beam from the PM fiber through a collimator. The F had a reflectivity of 99.2% for 1.55 μm at an $\sim$0° angle of incidence and a 97% transmission for the 2 μm *pump* laser used in this experiment to excite the gas particles. The near end of the GAC was sealed with an antireflection (AR, C-coating) coated BK7 wedge window (WW) to ensure least losses for the resonating ML laser beam. A distance of $\sim$5 mm between the WW and the fiber collimator was used to minimize the influence of ambient air on the measurements. The parameters of the ML *probe* laser were monitored via a photodiode (LabBuddy, DSC2-50S) connected to the tap of a 1% fiber coupler spliced into the resonator directly after the SESAM. The optical signal was additionally boosted by 15x in a custom erbium doped fiber amplifier before the photodiode.

The electric signal form the photodiode was delivered to a radio frequency (RF) spectrum analyzer (Rohde Schwarz FSW 43), which was capable of performing both analog and IQ demodulation at a chosen frequency. The tested gas sample was prepared by a commercial gas mixer (Environix, 4020) and forwarded directly to the GAC. In PTS techniques, the gas under test has to be excited to produce the PT effect, which

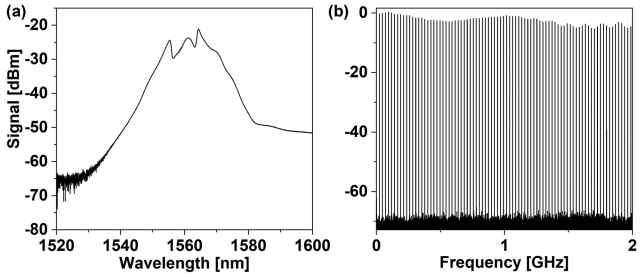

Fig. 2. (a) Optical spectrum of the ML emission plotted in a dBm scale. (b) Registered RF spectrum recorded for a 2 GHz span. All measurements were taken at the 1% tap output for 120 mW of pump power delivered to the active erbium-doped fiber and N_2 flowing through the GAC. The 2 μm *pump* was turned off.

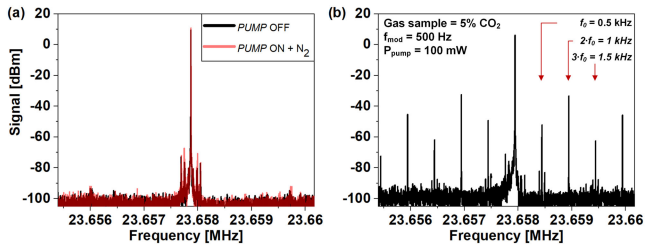

Fig. 3. Fundamental beatnote of the mode-locked laser registered for three cases. (a) Black trace – *pump* laser OFF; (a) Red trace – *pump* ON and N_2 in the GAC; (b) – *Pump* laser ON and the GAC filled with 5% CO_2. The characteristic modulation sidebands along with multiple harmonics are clearly visible when the gas is excited. Measurements were taken with 1 Hz bandwidth. Parameters of the *pump* laser are listed in the graph.

will then be detected by the *probe* laser. In this experiment, carbon dioxide (CO_2) molecules were used to determine the performance of the sensor. An isolated absorption line located at 4991.26 cm^{-1} ($\sim$2003.5 nm) was targeted by a tunable *pump* laser with a 100 mW maximum output power, which was formed by a distributed feedback laser (DFB, Eblana, EP2004) amplified in a custom-built fiber amplifier. The *pump* beam was coupled into the GAC through the F and precisely co-aligned with the 1.55 μm *probe* beam propagating inside it. The collimators were chosen so that both the *pump* beam and the *probe* beam had a similar $1/e^2$ diameter of $\sim$1.5 mm. All components were PM, thus self-starting of the ML operation was achieved each time by simply delivering 120 mW of *pump* power to the active fiber. Worth noting is the fact, that the *probe* sensor configuration is versatile and enables measuring any gas sample, at any wavelength, provided that an appropriate *pump* laser and beam-combining optics are used.

III. Mode-Locked *Probe* Laser Parameters

Firstly, parameters of the ML laser were examined, during which the GAC was flushed with pure nitrogen (N_2) and the *pump* laser was turned OFF, hence no modulation of the RI inside the ML laser cavity was present. Stable, self-starting ML operation of the *probe* laser is achieved each time the gain fiber is pumped with 120 mW from the 976 nm pump (note the difference between the 976 nm pump used for the Erbium gain fiber and the 2 μm *pump* used to excite the gas sample). Crucial parameters of the light emitted by the ML laser are shown in Fig. 2, and include the optical spectrum and the RF spectrum registered for a 2 GHz span.

The self-constructed ML laser operates at a center wavelength of 1560 nm, similarly to typical SESAM ML-fiber lasers. No signs of unstable dual-pulsing was observed. Due to the all-PM fiber configuration, once the mode-locked operation is achieved the laser could operate continuously as long as it is required by the experiments.

IV. Photothermal Gas Detection

To determine the performance of the proposed gas detection scheme CO_2 molecules were excited at the R18 line of the $2\nu1+\nu3$ band, located near 4991.26 cm^{-1}, which is clear of

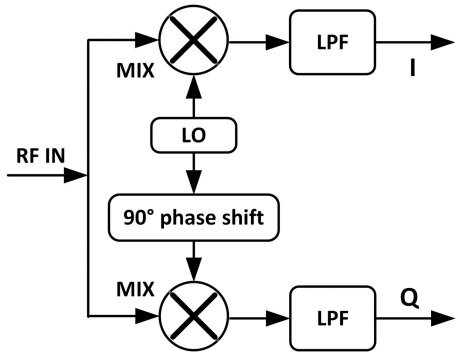

Fig. 4. Theory of IQ demodulation. MIX – RF mixer, LO – local oscillator, LPF – lowpass filters, I – in-phase components, Q – quadrature components.

water-vapor-related background absorption. The principle of operation of the described sensor is as follows. Due to the ML mechanism, thousands of longitudinal modes are phase locked in the cavity during the laser operation. There are several consequences of this effect. One is the emission of very short optical pulses, typically in the femtosecond range. Moreover, each of the laser longitudinal locked modes is separated from its neighbor by a fixed frequency value, which is directly connected with the cavity roundtrip, called also the pulse repetition frequency, which for linear cavity laser can be calculated as: $f_{rep} = c/(2L \cdot n)$, where c is the speed of light, L is the length of the resonator and n is the refractive index of the resonator. This results in generating characteristic beatnotes between the locked modes, starting from the fundamental beatnote at the f_{rep} and spanning up to hundreds of GHz (depending on the number of locked longitudinal modes), the so called frequency comb. This effect is illustrated in Fig. 2(b). The ML laser used in this experiment had a linear cavity with a length $\sim$4.3 m, thus the fundamental self-heterodyne beatnote signal was observed at $\sim$23.6 MHz. Any change in the optical length of the cavity is directly translated into an observable shift in the beatnote laser frequency - f_{rep}. According to the formula $f_{rep} = c/(2L \cdot n)$ this can be either related to a physical change in the resonator length (e.g., position of the F mirror in Fig. 1), or a change in the RI of the resonator. By placing a gas-filled cell inside the ML laser resonator we are able to exploit this effect to probe very small variations in the refractive index of the excited gas under test. The derivative of

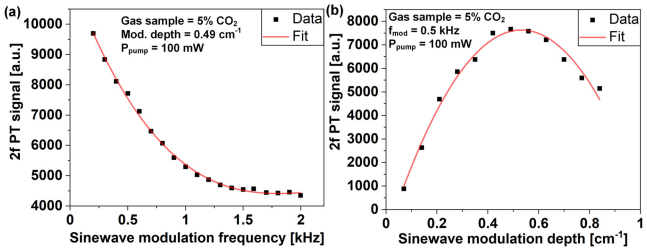

Fig. 5. Registered amplitude of the 2*f* PT signal plotted as a function of: (a) - the *pump* modulation frequency; (b) – the *pump* modulation depth. Measurement parameters are provided in the figures.

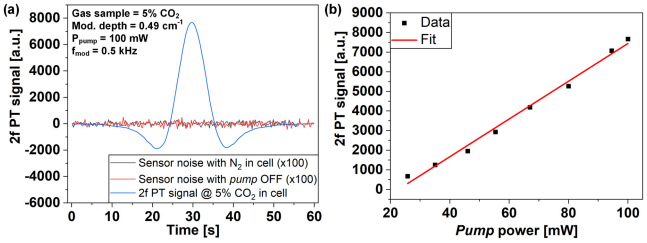

Fig. 6. (a) – full 2f scan across the CO_2 absorption line (blue trace). Sensor baseline noise measured for N_2 in the GAC (black trace) and for the *pump* laser turned OFF (red trace) are depicted with their amplitudes multiplied by 100 for clarity reasons. (b) – amplitude of the 2f PT signal plotted as a function of the *pump* power. Measurement parameters are provided in Figure (a).

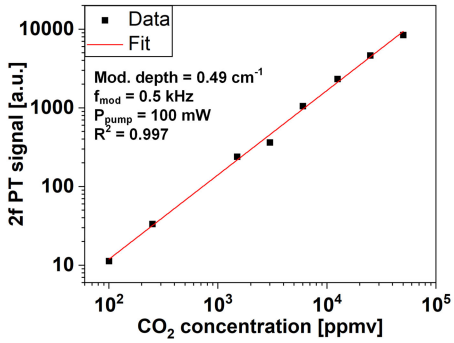

Fig. 7. Linearity of the sensor response for varying values of the CO_2 concentration. Measurement parameters are listed in the graph.

the $f_{rep} = c/(2L \cdot n)$ function in respect to a PT-induced change in the RI - Δn estimates the shift in the fundamental repetition frequency: $\Delta_{frep} = -(c \cdot \Delta n)/(2L \cdot n2)$. In this sensor, the gas sample is placed inside the ML laser cavity, therefore if the *pump* and *probe* beams are co-aligned in a GAC, any modulation of the gas RI will translate to changes in the pulse repetition frequency of the ML laser due to the correlation described by the equations above. By monitoring the frequency of the beatnote we can thus directly probe the change in the gas RI, which carries the information about its concentration. The proposed method allows directly translating the amplitude of the PTS signal to frequency deviations, which is highly desirable form the noise-limiting point of view. Worth noting is the fact, that in this particular case, the spectroscopic signal is automatically transcribed to deviations of a beatnote at 23.6578 MHz, taking all advantages from the 1/f noise limiting factor. The spectroscopic signal processing was additionally simplified by modulating the *pump* laser wavelength with a sinusoidal signal at f_0, which enabled us to use the WMS detection technique combined with phase sensitive lock-in-based signal acquisition [23]. To achieve this, the DFB laser diode used as the seed in the *pump* laser was mounted into a temperature and current controller (Thorlabs, CLD1015) and its injection current was controlled via a function generator (Tectronix, AFG3102) connected to the modulation input. To verify the influence of the photothermal-induced (PT) RI changes on the ML laser operation, the RF spectrum of the photodiode signal was registered for three cases: (I) with the *pump* laser OFF; (II) the *pump* laser ON at 100 mW and the GAC filled with pure N_2; (III) the *pump* laser ON at 100 mW and the GAC filled with 5% CO_2. During the measurements the wavelength of the *pump* laser was tuned to the center of the CO_2 absorption line. The results are plotted in Fig. 3.

The measurement in Fig. 3(b) clearly shows, that inducing the RI modulation in the CO_2 molecules trapped inside the cavity of the ML laser causes a measurable effect. The fundamental beatnote located at 23.6578 MHz exhibits a modulation, which frequency is related to the sinewave modulation of the *pump* laser. Characteristics sidebands, which are an indication of this effect appeared at the frequency $f_0 = 500$ Hz, as well as at its multiple harmonics ($2 \cdot f_0$, $3 \cdot f_0$, etc.), which is common for signals observed in the WMS technique [23]. On the other hand, with no gas in the gas cell, the *pump* laser did not introduce any observable residual modulation of the beatnote, which confirms, that a high signal-to-noise ratio (SNR) should be achievable.

To enable lock-in amplifier-based spectroscopic signal retrieval, the ML laser beatnote phase modulation had to be firstly demodulated, to extract the PT-induced RI modulation, which carries the information about the gas concentration. This was done by the use of an IQ- demodulator built into the RF spectrum analyzer, which monitored the electric signal delivered by the photodiode. The operation of an IQ-demodulator can be explained by representing its input signal $s_{RF}(t)$ as a combination of two double sideband modulated quadrature carriers [24]:

$$\begin{aligned} \boldsymbol{s_{RF}}(\boldsymbol{t}) &= \boldsymbol{s_I}(\boldsymbol{t}) + \boldsymbol{s_Q}(\boldsymbol{t}) \\ &= \boldsymbol{I}(\boldsymbol{t}) \cos \boldsymbol{\omega_{RF} t} - \boldsymbol{Q}(\boldsymbol{t}) \sin \boldsymbol{\omega_{RF} t} \end{aligned} \quad (2)$$

The illustration in Fig. 4 explains the principle used in IQ demodulators to extract the I and Q signals.

The input RF signal delivered by the photodiode is split and mixed with a local oscillator (LO) signal. In order to distinguish the I (in phase) and Q (quadrature) components the LO signal is phase shifted by 90° before one of the mixers. The mixer output signals are lowpass filtered to eliminate the high-frequency mixing products and thus providing only the baseband I and Q signals required for processing. Those signals carry the information about the frequency and phase modulation of the input RF signal. In this experiment the IQ demodulation was performed digitally by the RF spectrum analyzer software and the resulting ML laser beatnote phase modulation was calculated and extracted from the apparatus using a custom developed LabView software running on a standard personal computer (PC). Note that commercial IQ demodulators can also be used for this purpose. The photodiode signal was demodulated with

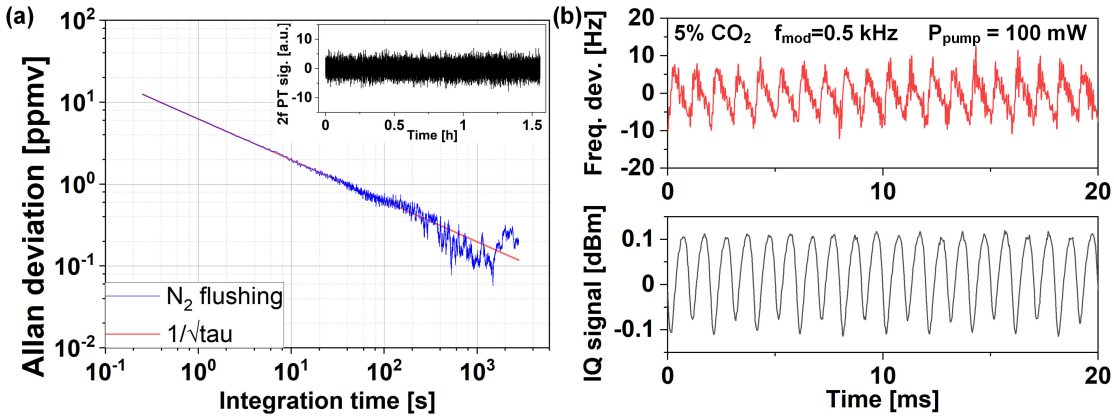

Fig. 8. (a) Allan deviation plot calculated for ppmv values on the Y-axis. The inset shows the noise signal registered after filling the GAC with N_2, which was used to calculate the Allan plot. (b) raw analog demodulator signal and (c) raw IQ demodulator signal registered for the GAC filled with 5% CO_2. Plots (b) and (c) were registered for 5% CO_2 in the GAC, 35 kHz BW of the demodulators and for *pump* parameters as listed in the graph.

a bandwidth (BW) of 35 kHz at the fundamental beatnote of the ML laser located at $\Omega = 23.6578$ MHz. The LabView application calculated the Fast Fourier Transform (FFT) of the demodulated signal and plotted the amplitudes of f_0 harmonics as a function of time. This feature allowed us to, e.g., analyze the amplitude of the second harmonic of the beatnote phase modulation, similarly to traditional WMS detection. The most crucial parameters of the WMS-based detection scheme, which are the *pump* modulation frequency and depth were optimized to obtain the highest possible amplitude of the spectroscopic signal and the lowest level of the background noise. Graphs showing the amplitudes of the second harmonic PT signal plotted for several setpoints of the abovementioned values are shown in Fig. 5.

Based on the measurements, the optimal *pump* modulation depth was chosen at a value of 0.49 cm^{-1}, which was defined using the approach described in [22]. The amplitude of the 2f PT signal decreases at higher values of the *pump* modulation frequency (f_0), which is caused by the limited gas molecule relaxation time [6]. Low values of the f_0 will produce higher signals, however, the sensor will be prone to mechanical, acoustic and 1/f noise pickup. The optimal value of this parameter is dependent on the configuration of the sensor itself. In case of the presented sensor setup the highest SNR was obtained for the f_0 value of 500 Hz. The experimentally determined values will be used in the following measurements. To present the full 2f scan of the CO_2 absorption profile an additional 60 s sawtooth ramp was superimposed onto the sinewave modulation signal of the *pump* seed. The measured signal is presented in Fig. 6(a).

The registered 2f signal clearly shows the characteristic absorption profile of the measured gas sample. No significant fringe-related noise was observed in the measured signal. Maximum signal amplitude for a 5% CO_2 gas sample was 7705, and was limited by the *pump* laser power. We have also measured the baseline noise of the sensor. This was realized by flushing the GAC with N_2 and sweeping the wavelength of the *pump* across the same spectral range, as it was performed during the full 2f scan of the absorption line. This analysis confirms that the proposed PT gas detection method is free from baseline noise, commonly found in traditional detection methods, e.g., based on tunable diode laser absorption spectroscopy (TDLAS). According to equation (1), the optically induced PT effect and the resulting RI modulation is linearly proportional to the optical power of the *pump* laser. This relationship was verified in our sensor by changing the optical power of the *pump* laser exciting the gas molecules in the GAC. The obtained results plotted in Fig. 5(b) confirm, that the response of the sensor could be fitted using a linear function and that the sensor performs similarly to other PTS-aided gas detectors [17], [25], [26]. The linearity of the sensor response was also verified for various concentrations of the analyte gas. The results are plotted in Fig. 7.

For this test, the GAC was filled with CO_2 mixtures with concentrations ranging from 100 parts-per-million by volume (ppmv) to 5%, which were prepared using a commercial gas mixing system. During the measurement, the *pump* laser was tuned to the center of the CO_2 absorption line and the modulation parameters were set as listed in the graph. The maximum 2f PT signal values for each concentration were measured after fully flushing the GAC. The obtained R^2 value was 0.997, which is comparable to other PTS gas sensors [14], [19], [21]. To estimate the sensor performance we have measured the sensor noise with 20 Hz sampling rate for 100 minutes, while the GAC was flushed with N_2. The registered values were used to calculate and plot the Allan deviation function, as presented in Fig. 8. During the measurement the *pump* laser was tuned to the center of the CO_2 absorption line and the modulation parameters were set as for previous experiments.

Based on the Allan deviation analysis of the sensor noise a minimum detection limit (MDL) equal to 6.2 ppmv and 636 parts-per-billion by volume (ppbv), for 1 s and 100 s integration times, respectively, were obtained. Due to the unique PTS signal retrieval method, the concentration of the gas analyte is encoded directly into frequency deviations. Therefore, the registered spectroscopic signal is highly invulnerable to variation of the optical signal amplitude reaching the photodiode used to probe the signal, thus the noise in the sensor is dominated in majority by 1/f noise. This means that the registered spectroscopic signal can be averaged even for 1000 s, reaching a 111 ppbv MDL. The obtained MDL is 46 times better, when compared to

our previous, less versatile configuration [13]. This is a direct result of two key improvements: using a novel sensor layout, in which the ring cavity was substituted with a linear cavity and switching from analog beatnote frequency demodulation to IQ phase demodulation. A direct comparison of the raw demodulated signals for analog demodulation (Fig. 8(b)) and IQ demodulation (Fig. 8(c)) reveals the significant improvement in terms of noise contribution for the latter case (both signals were registered for equal bandwidth filter setting of 35 kHz). Note that the analog demodulated signal is presented only to demonstrate the substantial improvement in terms of noise contribution in the extracted signal when using IQ demodulation.

TABLE I
PERFORMANCE OF SELECTED PT GAS SENSORS

Gas	Detection method	λ	Cell length	NEA	Integration time
N_2O [25]	HCF-FPI	3.6 μm	120 cm	$3.0{\cdot}10^{-5}$	40 s
Ethane [8]	HCF-FPI	3.34 μm	14 cm	$3.5{\cdot}10^{-6}$	100 s
SO_2 [26]	FPI	7.2 μm	1 mm	$1.8{\cdot}10^{-6}$	1 s
CO_2 [13]	ML-PT	2 μm	10 cm	$7.19{\cdot}10^{-5}$	1 s
				$2.48{\cdot}10^{-6}$	100 s
CO_2 (this work)	LC-ML-PT	2 μm	20 cm	$1.23{\cdot}10^{-5}$	1 s
				$1.26{\cdot}10^{-6}$	100 s
				$2.25{\cdot}10^{-7}$	1000 s

V. CONCLUSION AND OUTLOOK

In this paper, a novel configuration of a gas sensor was demonstrated, which documents a unique technique of probing the PT-induced RI modulation. Here, the *probe* part of the sensor is based on a simple, linear cavity SESAM ML fiber laser. In comparison to our previous version of the sensor [13], the re-designed version contains less fiber components, is easier to align and provides better versatility. A custom built, 20 cm-long gas absorption cell was incorporated inside the ML laser resonator and enabled simple gas sample testing. CO_2 molecules having a strong transition near 4991.26 cm^{-1} were chosen as the target gas sample. The gas was excited by a *pump,* which was a custom-built tunable laser that was coupled in the counter-propagating direction into the GAC through an optical component serving as a mirror for the ML laser cavity and co-aligned with the resonating *probe* beam. The induced RI modulation affected the optical-path length of the ML laser cavity, modulating the phase of its beatnotes. This unique approach to PTS signal retrieval leads to a direct translation of the spectroscopic signal to the frequency deviation, a technique highly desirable from metrological and noise-immunity point of view. The beatnote phase was retrieved via IQ demodulation and the analysis of the spectroscopic signal encoded therein was significantly simplified by implementing the WMS technique, which only required applying a sinusoidal modulation of the *pump* wavelength with optimized parameters. A custom LabView application was used to aggregate and plot the results of the measurements. The performance of the sensor was optimized and subsequently evaluated by performing zero-gas Allan deviation analysis. Although having a non-complex layout, the proposed sensor configuration reached a minimum detectable CO_2 concentration of 6.2 ppmv, 636 ppbv and 111 ppbv, for 1 s, 100 s and 1000 s, respectively. These values correspond to a noise equivalent absorption (NEA) of $1.23{\cdot}10^{-5}$, $1.26{\cdot}10^{-6}$ and $2.25{\cdot}10^{-7}$ for 1 s, 100 s and 1000 s, respectively. This is comparable or superior to PTS gas detectors having a more complex layout [8], [20], [27]. The long averaging time achievable in the presented, unique configuration is applicable due to the purely frequency-based signal retrieval, in which the white noise is a dominant source of the parasitic signal. The results show more than an order of magnitude increase in the MDL, when compared to the previously presented architecture of the ML PTS gas sensor [13]. This was achieved by re-designing the *probe* laser to work in a linear cavity, instead of a ring resonator. Here, the induced RI modulation induces a two-fold higher effect on the ML laser beatnote phase, according to the equation $\Delta f_{rep} = c/(2L(n + \Delta n)$, where f_{rep} is the repetition frequency of the ML laser, c is the light speed, L is the length of the resonator, n is the resonator RI and Δn is the *pump* induced RI modulation inside the ML laser resonator. Moreover, as presented in Fig. 8(b) and (c), a significant improvement in terms of the noise contribution was achieved by IQ demodulation of the beatnote phase, rather than using a simple analog demodulation approach. On top of that, the improved layout of the ML PT sensor simplifies the co-alignment of the *pump* beam and the *probe* beam, which in the next iteration will allow coupling several auxiliary lasers and performing simultaneous multi species detection. A comparison of the performance of several PT gas sensors is provided in Table I. The proposed method of RI modulation readout is versatile and can be used to sample any type of gas, provided an appropriate optical component is used in the GAC (element F in Fig. 1). This component has to serve as the second mirror of the linear cavity of the ML laser and simultaneously transmit the pump laser beam, which induces the RI modulation. Worth noting is the fact, that the ML laser can be constructed to work at any wavelength – e.g., 1 μm or 2 μm. The characteristics of the ML emission are not crucial, as long as the emission is stable and self-starting of the pulsed operation occurs after turning the laser ON. Here we have chosen 1.55 μm as the telecom fiber components are inexpensive and widely available. In order to maximize the observable phase change amplitude the optical pathlength in which the RI modulation occurs should be elongated, compared to the total length of the ML laser resonator. Due to the unique mechanism of the sensor readout, which allows encoding the spectroscopic signal into frequency deviations, the long averaging times can be used to achieve satisfactory minimum detection limits. The main limiting factor of the sensor's sensitivity was the accuracy of the IQ demodulator used to decode the phase modulation. Significant improvement could be achieved if modules having superb performance would be incorporated.

We believe, that further development of novel types of PT gas sensors employing the ML fiber laser phase readout can lead to obtaining detection limits comparable with complex state-of-the-art detectors while maintaining compactness and versatility.

REFERENCES

[1] Y. Ma, A. Vicet, and K. Krzempek, "State-of-the-Art laser gas sensing technologies," *Appl. Sci.*, vol. 10, 2020, Art. no. 433, doi: 10.3390/app10020433.

[2] B. Fu *et al.*, "Recent progress on laser absorption spectroscopy for determination of gaseous chemical species," *Appl. Spectrosc. Rev.*, vol. 57, pp. 1–41, 2020, doi: 10.1080/05704928.2020.1857258.

[3] R. Müller *et al.*, "Thermoelectrically-Cooled InAs/GaSb Type-II superlattice detectors as an alternative to HgCdTe in a real-time mid-infrared backscattering spectroscopy system," *Micromachines*, vol. 11, 2020, Art. no. 1124, doi: 10.3390/mi11121124.

[4] P. Kalinowski, J. Miko\lajczyk, A. Piotrowski, and J. Piotrowski, "Recent advances in manufacturing of miniaturized uncooled IR detection modules," *Semicond. Sci. Technol.*, vol. 34, 2019, Art. no. 033002, doi: 10.1088/1361-6641/aaf458.

[5] C. L. Tan and H. Mohseni, "Emerging technologies for high performance infrared detectors," *Nanophotonics*, vol. 7, pp. 169–197, 2018, doi: 10.1515/nanoph-2017-0061.

[6] S. E. Bialkowski, N. G. C. Astrath, and M. A. Proskurnin, *Photothermal Spectroscopy Methods*. Wiley, 2019.

[7] C. C. Davis and S. J. Petuchowski, "Phase fluctuation optical heterodyne spectroscopy of gases," *Appl. Opt.*, vol. 20, pp. 2539–2554, 1981, doi: 10.1364/AO.20.002539.

[8] F. Chen *et al.*, "Ethane detection with mid-infrared hollow-core fiber photothermal spectroscopy," *Opt. Exp.*, vol. 28, pp. 38115–38126, 2020, doi: 10.1364/OE.410927.

[9] J. P. Waclawek, H. Moser, and B. Lendl, "Balanced-detection interferometric cavity-assisted photothermal spectroscopy employing an all-fiber-coupled probe laser configuration," *Opt. Exp.*, vol. 29, pp. 7794–7808, 2021, doi: 10.1364/OE.416536.

[10] J. P. Waclawek, C. Kristament, H. Moser, and B. Lendl, "Balanced-detection interferometric cavity-assisted photothermal spectroscopy," *Opt. Exp.*, vol. 27, pp. 12183–12195, 2019, doi: 10.1364/OE.27.012183.

[11] K. Krzempek *et al.*, "Multi-pass cell-assisted photoacoustic/photothermal spectroscopy of gases using quantum cascade laser excitation and heterodyne interferometric signal detection," *Appl. Phys. B.*, vol. 124, 2018, Art. no. 74, doi: 10.1007/s00340-018-6941-x.

[12] K. Krzempek, G. Dudzik, K. Abramski, G. Wysocki, P. Jaworski, and M. Nikodem, "Heterodyne interferometric signal retrieval in photoacoustic spectroscopy," *Opt. Exp.*, vol. 26, pp. 1125–1132, 2018, doi: 10.1364/OE.26.001125.

[13] K. Krzempek, G. Dudzik, and K. Abramski, "Photothermal spectroscopy of CO2 in an intracavity mode-locked fiber laser configuration," *Opt Exp.*, vol. 26, pp. 28861–28871, 2018, doi: 10.1364/OE.26.028861.

[14] G. Dudzik, K. Krzempek, K. Abramski, and G. Wysocki, "Solid-state laser intra-cavity photothermal gas sensor," *Sensors Actuators B: Chem*, vol. 328, 2021, Art. no. 129072, doi: 10.1016/j.snb.2020.129072.

[15] K. Krzempek, P. Jaworski, P. Kozioł, and W. Belardi, "Antiresonant hollow core fiber-assisted photothermal spectroscopy of nitric oxide at 5.26 μm with parts-per-billion sensitivity," *Sensors Actuators B: Chem.*, vol. 345, 2021, Art. no. 130374, doi: 10.1016/j.snb.2021.130374.

[16] P. Zhao *et al.*, "Mode-phase-difference photothermal spectroscopy for gas detection with an anti-resonant hollow-core optical fiber," *Nature Commun.*, vol. 11, 2020, Art. no. 847, doi: 10.1038/s41467-020-14707-0.

[17] K. Krzempek, "A review of photothermal detection techniques for gas sensing applications," *Appl. Sci.*, vol. 9, 2019, Art. no. 2826, doi: 10.3390/app9142826.

[18] C. Yao *et al.*, "Photothermal CO detection in a hollow-core negative curvature fiber," *Opt. Lett.*, vol. 44, pp. 4048–4051, 2019, doi: 10.1364/OL.44.004048.

[19] Z. Li, Z. Wang, F. Yang, W. Jin, and W. Ren, "Mid-infrared fiber-optic photothermal interferometry," *Opt. Lett.*, vol. 42, pp. 3718–3721, 2017, doi: 10.1364/OL.42.003718.

[20] J. P. Waclawek, V. C. Bauer, and H. Moser, and B. Lendl, "2*f*-wavelength modulation Fabry-Perot photothermal interferometry," *Opt. Exp.*, vol. 24, pp. 28958–28967, 2016, doi: 10.1364/OE.24.028958.

[21] C. Yao, S. Gao, Y. Wang, P. Wang, W. Jin, and W. Ren, "MIR-pump NIR-probe fiber-optic photothermal spectroscopy with background-free first harmonic detection," *IEEE Sensors J.*, vol. 20, no. 21, pp. 12709–12715, Nov. 2020, doi: 10.1109/JSEN.2020.3000795.

[22] K. Krzempek, P. Jaworski, P. Kozioł, and W. Belardi, "Antiresonant hollow core fiber-assisted photothermal spectroscopy of nitric oxide at 5.26 μm with parts-per-billion sensitivity," *Sensors Actuators B: Chem.*, vol. 345, 2021, Art. no. 130374, doi: 10.1016/j.snb.2021.130374.

[23] J. M. Supplee, E. A. Whittaker, and W. Lenth, "Theoretical description of frequency modulation and wavelength modulation spectroscopy," *Appl. Opt.*, vol. 33, pp. 6294–6302, 1994, doi: 10.1364/AO.33.006294.

[24] C. Ziomek and P. Corredoura, "Digital I/Q demodulator," in *Proc. Part. Accel. Conf.*, 1995, vol. 4, pp. 2663–2665. doi: 10.1109/PAC.1995.505652.

[25] H. Bao *et al.*, "Modeling and performance evaluation of in-line Fabry-Perot photothermal gas sensors with hollow-core optical fibers," *Opt. Exp.*, vol. 28, pp. 5423–5435, 2020, doi: 10.1364/OE.385670.

[26] W. Jin, Y. Cao, F. Yang, and H. L. Ho, "Ultra-sensitive all-fibre photothermal spectroscopy with large dynamic range," *Nature Commun.*, vol. 6, 2015, Art. no. 6767, doi: 10.1038/ncomms7767.

[27] C. Yao, S. Gao, Y. Wang, P. Wang, W. Jin, and W. Ren, "Silica hollow-core negative curvature fibers enable ultrasensitive mid-infrared absorption spectroscopy," *J. Lightw. Technol.*, vol. 38, no. 7, pp. 2067–2072, Apr. 2020, doi: 10.1109/JLT.2019.2960804.

Karol Krzempek received the Ph.D. degree in nonlinear frequency conversion-based mid-infrared laser sources from the Faculty of Electronics, Wroclaw University of Science and Technology (WUST), Wrocław, Poland, in 2016. He is currently continues his research in this area with WUST, where he founded the Laser Spectroscopy Group (LSG). He participated in 14 research grants (four as Principal Investigator), and is the coauthor of 11 national patents. His main research interests include design and optimization of CW and pulsed fiber-based laser sources working in the 1 μm, 1.5 μm and 2 μm wavelength regions and subsequent nonlinear mixing of the emission of such coherent sources. His research interests also include sensors relying on photothermal gas detection techniques, and also efficient use of hollow-core fibers as low-volume gas cells in laser spectroscopy applications. Throughout his academic career, he was the recipient of numerous national scholarships and awards. Recently, he contributed to more than 100 scientific works and was the coeditor of *MDPI and Frontiers in Physics*.

Piotr Jaworski received the Ph.D. degree in physics from Heriot-Watt University, Edinburgh, U.K., in 2015. During the Ph.D. studies, he was working on the development of novel antiresonant hollow-core fibers for the delivery of high peak power pulsed laser light in the near-ir and visible spectral range and its application to precision micro-machining. In 2015, he joined Lukasiewicz Research Network - PORT Institute (before Wroclaw Research Center EIT+), as a Research Engineer with Laser Sensing Laboratory. Since then, his research work has been focused on laser-based gas sensing using both bulk optics-based and hollow-core fibers-based gas spectrometers. In 2018, he became the Head of Laser Sensing Laboratory, PORT. In 2019, he joined the Laser Spectroscopy Group, Wroclaw University of Science and Technology, focusing his research on gas sensing using hollow-core microstructured fibers. He is the author and coauthor of 42 research articles, conference proceedings, and conference presentations. He is a main investigator in eight research projects and principal investigator in one research grant. He also developed two laser-based gas sensing systems for industrial enterprises from Poland.

Piotr Bojęś is currently working toward the Ph.D. degree with **KK** Research Group, Wroclaw University of Science and Technology, Wrocław, Poland. He is the author of two research papers and numerous conference presentations. His research interests include computer-based simulations, hollow-core fiber-based laser spectroscopy, photothermal spectroscopy, and photoacoustic spectroscopy.

Paweł Kozioł received the Ph.D. degree in telecommunication from the Wroclaw University of Science and Technology, Wroclaw, Poland, in 2017. During the Ph.D. studies, he was working on the development of the technology of direct laser metallization of the ceramic surface and its application in fabrication of passive metamaterial structures for the microwave and terahertz range. In 2015, he joined Lukasiewicz Research Network – PORT Institute (prior Wroclaw Research Center EIT+), as a Research Engineer with Laser Micromachining Laboratory. Since then, his research work has been focused on laser modification and material processing using ns, ps lasers for different applications (mainly for industry). In 2019, he joined the Laser Spectroscopy Group, Wroclaw University of Science and Technology, focusing his research on integration of sensitive methods of detecting trace concentrations of gases with sensor systems based on low-loss microstructural optical fibers with an air core. He is the coauthor of 33 research articles, conference proceedings and conference presentations. He was the Principal Investigator in one research grant and the main investigator in four research projects.